



Highly Time-Resolved Measurements of Secondary Ions in PM_{2.5} during the 2008 Beijing Olympics: The Impacts of Control Measures and Regional Transport

Xiaomei Gao^{1,2}, Wei Nie^{1,2}, Likun Xue², Tao Wang^{1,2,3}, Xinfeng Wang^{1,2}, Rui Gao¹, Wenxing Wang^{1,3*}, Chao Yuan^{1,2}, Jian Gao³, Kant Pathak Ravi², Jing Wang¹, Qingzhu Zhang¹

¹ Environment Research Institute, Shandong University, Jinan 250100, China

² Department of Civil and Structural Engineering, The Hong Kong Polytechnic University, Hong Kong, China

³ Chinese Research Academy of Environmental Sciences, Beijing 100012, China

ABSTRACT

Highly time-resolved measurements of SO₄²⁻, NO₃⁻, and NH₄⁺ in PM_{2.5} were simultaneously performed at an urban site and downwind rural site in Beijing during the 2008 Olympics to investigate the impacts of control measures and regional transport. The mean concentrations (± standard deviations) of SO₄²⁻, NO₃⁻, and NH₄⁺ were 18.23 (± 19.96), 9.47 (± 11.41), and 9.70 (± 8.92) μg/m³, respectively, at the rural site. These concentrations were comparable to those of 20.74 (± 20.36), 8.83 (± 9.51), and 10.85 (± 8.99) μg/m³ at the urban site. Clear diurnal variations of SO₄²⁻, NO₃⁻, and NH₄⁺ were observed at both sites, and were related to meteorological conditions, primary emissions, and regional transport. The effectiveness of the control measures on SO₄²⁻, NO₃⁻, and NH₄⁺ was evaluated by comparing the urban site concentrations during three periods: before the full-scale control, after the full-scale control but before the Olympics, and during the Olympics. The high pollution observed after the full-scale control was attributed to regional transport from the sector south of Beijing. The samples in the air masses from the northwest were selected to minimize the influences of meteorological factors and regional transport, and the results showed a clear reduction of SO₄²⁻, NO₃⁻, and NH₄⁺ concentrations (approximately 35%–69%) after the full-scale control began, suggesting the effectiveness of the control measures in reducing the local secondary inorganic aerosols. A widespread pollution episode was observed during August 3–10 at the rural site, with regional transport being identified as the main contributor. Secondary transformation evidently occurred during August 3–4 and contributed more than 50% of the rural secondary ion concentrations. During August 5–10, the whole region experienced a stable and well-developed plume.

Keywords: Highly time-resolved; Secondary ions in PM_{2.5}; Olympic Games; Beijing; Regional transport.

INTRODUCTION

Fine particles (PM_{2.5}, particulate matter with an aerodynamic diameter smaller than or equal to 2.5 μm) play key roles in regional air quality deterioration and global climate change (Sloane *et al.*, 1991; Deshmukh *et al.*, 2011), and they can easily penetrate into the lungs and lead to respiratory and mutagenic diseases (Hughes *et al.*, 1998). The secondary species such as sulfate, nitrate, and ammonium are the major PM_{2.5} compounds, accounting for more than 1/3 of the PM_{2.5} mass (Zhang *et al.*, 2007; Chan and Yao, 2008). These species can affect the hygroscopic nature and acidity of aerosols (Ocskay *et al.*, 2006). Therefore, understanding the temporal/spatial variations of the secondary species in

PM_{2.5} is important.

Beijing, as the capital of China, is situated in one of the fastest developing regions of the North China Plain (NCP). Due to the high primary emission levels from fossil fuel consumption, Beijing has experienced serious air pollution problems, especially particulate matter pollution (Chan and Yao, 2008; Yang *et al.*, 2011). PM_{2.5} concentrations much higher than the ambient air quality standard of 35 μg/m³ recommended by the United States Environmental Protection Agency (US-EPA) have been reported (e.g., He *et al.*, 2001; Wang *et al.*, 2005; Duan *et al.*, 2006; Wang *et al.*, 2008; Zhou *et al.*, 2012). Therefore, numerous studies have been conducted in Beijing to investigate the properties of PM_{2.5} and the formation mechanism of secondary species. For example, He *et al.* (2001) and Duan *et al.* (2006) reported the seasonal variations and chemical compositions of PM_{2.5}, and the results showed the highest concentrations of PM_{2.5} in winter and the major components of carbonaceous species (the sum of OC and EC), secondary ions (the sum of SO₄²⁻, NO₃⁻, and NH₄⁺), and crustal species. Yao *et al.* (2002)

* Corresponding author. Tel.: 0531-88369788;
Fax: 0531-88361990
E-mail address: wenxwang@hotmail.com

attributed the SO_4^{2-} formation to gas-phase oxidation in winter but to in-cloud processes in summer, while Sun *et al.* (2006) suggested that the aqueous-phase oxidation of SO_2 was the major mechanism of SO_4^{2-} formation in winter. However, most previous studies on the chemical characteristics of $\text{PM}_{2.5}$ were based on the off-line filter sampling method, which has several shortcomings, such as low time resolution and sampling artifacts from the dissociation of semi-volatile species and inter-particle/gas-particle interactions (e.g., Pathak *et al.*, 2009; Nie *et al.*, 2010). To overcome these drawbacks, recently developed highly time-resolved techniques for measuring water soluble ions in $\text{PM}_{2.5}$ (or PM_{10}) have been applied to provide more accurate and detailed information about the chemical processes (e.g., Takegawa *et al.*, 2009; Sun *et al.*, 2010; Gao *et al.*, 2011). However, to our knowledge, the studies involving these improved techniques have been limited to Beijing.

After winning the bid to host the 29th Olympic Games, the Beijing government took drastic actions to reduce air pollutant emissions and improve air quality. SO_2 , NO_x , and PM_{10} emissions were reduced by an estimated 14%, 38%, and 20%, respectively (UNEP, 2010). This dramatic emission reduction in a short period of time has attracted numerous studies to assess the impacts of control measures on the air quality. Based on comparisons of the data obtained during the Olympics with those from non-Olympic periods, the levels of SO_2 , NO_x , and PM_{10} were reduced by 40%–70%, 40%–50%, and 35%–55%, respectively (Wang *et al.*, 2009a, b, 2010a; Zhou *et al.*, 2010a). Compared to 2008, reductions of 43%, 13%, and 12% for NO_2 , SO_2 , and CO were reported over Beijing and neighboring provinces by satellite measurement (Witte *et al.*, 2009), and SO_2 and CO were reduced by 64% and 27% at Heishanzhai (HSZ) (Wang *et al.*, 2010b) and 60% and 32% at Miyun according to the field observations (Wang *et al.*, 2009b). The secondary ions in $\text{PM}_{2.5}$ (SO_4^{2-} , NO_3^- , and NH_4^+) had varied responses to the control measures and were influenced by both emissions and meteorological variations (Wang *et al.*, 2009c; Huang

et al., 2010; Okuda *et al.*, 2011; Xing *et al.*, 2011). However, the relative contributions of the emission reductions and meteorological factors to the air quality improvement during the Olympics remain inconclusive.

In the present study, highly time-resolved measurements of SO_4^{2-} , NO_3^- , and NH_4^+ in $\text{PM}_{2.5}$ were simultaneously performed at an urban site and a rural site in Beijing during the 29th Olympics. We first investigated the spatial and diurnal variations of SO_4^{2-} , NO_3^- , and NH_4^+ based on their hourly concentrations. To directly estimate the effectiveness of the control measures on the secondary ions, the air masses from northwestern Beijing were selected to minimize the influences of meteorological factors and regional transport. Finally, we analyzed a typical regional haze episode with high concentrations of SO_4^{2-} , NO_3^- , and NH_4^+ and emphasized the regional contribution, especially the transformation during transport. To our knowledge, this work is the first application of continuous techniques for simultaneously measuring water-soluble ions at an urban site and a downwind rural site in Beijing.

EXPERIMENT

Sampling Sites

The field campaign took place at an urban site and a rural site in Beijing in the summer of 2008 (shown in Fig. 1). The rooftop of a three-floor building was selected as the urban site (~15 m above the ground) in the Chinese Research Academy of Environmental Sciences (CRAES), which is 5.8 km south of the Olympic Stadium (the “Bird’s Nest”) and 4 km north of the 5th Ring Road. The rural site was situated in Heishanzhai (HSZ), approximately 40 km from CRAES. Detailed information about the two sites can be found in Wang *et al.* (2010b), and the sampling inlet was approximately 1.5 m above the rooftop of the station. The hourly data of SO_4^{2-} , NO_3^- , and NH_4^+ in $\text{PM}_{2.5}$ were collected from July 11 to August 25 at the urban site and from July 31 to August 25 at the rural site.

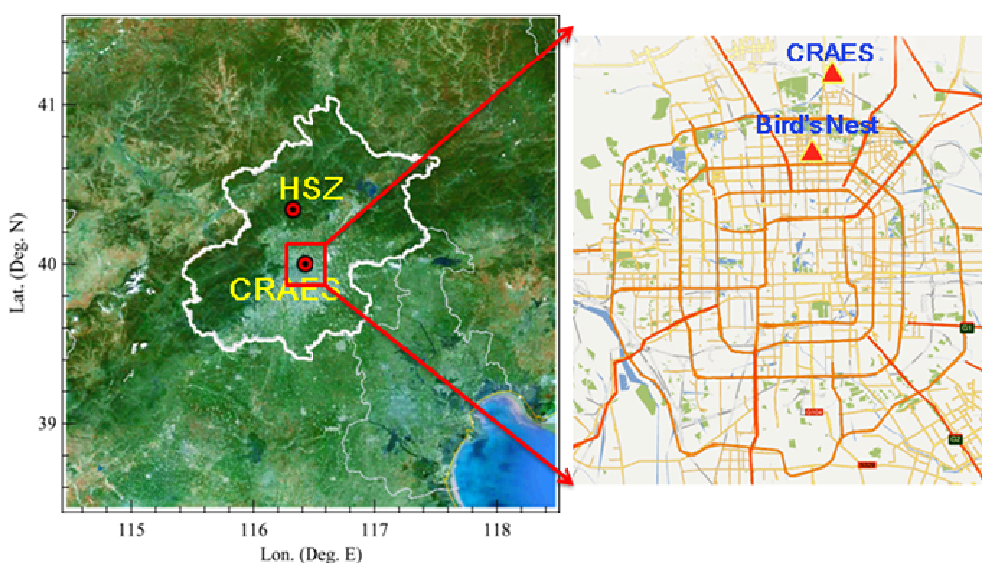


Fig. 1. Location of the two sites in Beijing.

Instruments Description

The hourly concentrations of SO_4^{2-} , NO_3^- , and NH_4^+ in $\text{PM}_{2.5}$ were simultaneously measured by two separate ambient ion monitors (AIM; Model URG 9000B, URG Corporation, USA) at both sites. These instruments contain two parts: a $\text{PM}_{2.5}$ sampler and a water-soluble ion analyzer. The ambient air was drawn through a 2.5 μm cut-point cyclone to remove particles larger than 2.5 μm from the air stream at a flow rate of 3 L/min followed by a Liquid Diffusion Denuder where de-ionized water flowed in the opposite direction of the air flow to remove the potential interfering gases (e.g., SO_2 , NH_3 , and HNO_3). The flow passed through an Aerosol Super-Saturation Chamber in which air stream rapidly mixed with the super-saturated steam to enhance particle growth into droplets. The solutions of water-soluble ions were collected in two syringes and then analyzed using two ion chromatography systems (Dionex, ICs 90 at CRAES, and ICs 1000 at HSZ). Multi-point calibrations were performed every four days after changing the eluent solutions. The estimated detection limits of SO_4^{2-} , NO_3^- , and NH_4^+ were 0.054, 0.010, and 0.045 $\mu\text{g}/\text{m}^3$, respectively, and the measurement uncertainties were approximately 10% (Zhou et al., 2010b). To avoid interference from high SO_2 and aerosol loadings, which were found in our previous studies (Wu and Wang, 2007; Zhou et al., 2010b), the sampling flow rate was reduced from 3 L/min to 2 L/min by adding a bypass before the inlet of the denuder; as a result, these two instruments performed well during our entire campaign (Nie et al., 2010).

Other instruments for measuring SO_2 (TEI model 43C), NO_x (TEI model 42i), O_3 (TEI model 49i), and CO (API model 300E or API model 300EU) were described in our previous papers (e.g., Wang et al., 2010b).

RESULTS AND DISCUSSIONS

Overall Results: Concentrations of SO_4^{2-} , NO_3^- , and NH_4^+ at the Two Sites

To obtain the spatial patterns of SO_4^{2-} , NO_3^- , and NH_4^+ in $\text{PM}_{2.5}$, we compared their concentrations at the two sites based on the data from July 31 to August 25. The results are summarized in Table 1, which shows the values of SO_2 , NO_x , temperature (T), relative humidity (RH), and solar radiation. A t-test (Microsoft Office Excel 2007) was also employed to evaluate the differences in the above parameters

at the two sites. The mean concentrations of SO_4^{2-} , NO_3^- , and NH_4^+ were 18.23 ± 19.96 , 9.47 ± 11.41 , and 9.70 ± 8.92 $\mu\text{g}/\text{m}^3$, respectively, at HSZ and were comparable to those at CRAES (20.74 ± 20.36 , 8.83 ± 9.51 , and 10.85 ± 8.99 $\mu\text{g}/\text{m}^3$, respectively). No significant difference was observed between these two sites, with mean concentration deviations less than 10%, as is consistent with previous studies. He et al. (2001) found that the levels of SO_4^{2-} , NO_3^- , and NH_4^+ showed little differences when measured at residential and downtown sites. Wang et al. (2005) compared the concentrations of SO_4^{2-} , NO_3^- , and NH_4^+ in five urban and rural areas using the paired samples t-test and concluded that there were no significant differences in their concentrations.

Unlike ions, the mean mixing ratios of SO_2 and NO_x (the precursors of SO_4^{2-} and NO_3^- , respectively) showed large differences at the two sites. The levels of SO_2 and NO_x at CRAES (7.25 ± 5.32 and 12.89 ± 9.75 ppb, respectively) were approximately 6 and 5 times those measured at HSZ (1.27 ± 1.47 and 2.51 ± 1.90 ppb), respectively, with p values < 0.01 at the 95% confidence level. The elevated SO_2 and NO_x levels at CRAES are likely due to the high traffic density and industrial emissions around or upwind of CRAES. Significant differences for the temperature, solar radiation, and relative humidity (Table 1) at the two sites were also observed, with p values < 0.01 at the 95% confidence level. The obvious differences in gas precursors and weather conditions as well as the similarities of the secondary inorganic ion levels suggested a more regional dependence for the secondary inorganic ions than that of the primary gases.

Overall Results: Diurnal Variations of SO_4^{2-} , NO_3^- , and NH_4^+

The diurnal variations of SO_4^{2-} , NO_3^- , and NH_4^+ in $\text{PM}_{2.5}$ and related trace gases (SO_2 and O_3), as well as the meteorological conditions (T, RH, and wind speed and direction), from July 31 to August 25 at the two sites are shown in Fig. 2. On the whole, SO_4^{2-} showed similar diurnal patterns at both sites with a broad daytime maximum and a relatively low concentration at night. The SO_4^{2-} concentrations rapidly increased from the early morning to the late afternoon synchronously with the enhancement of solar radiation and the O_3 and SO_2 concentrations. However, a more pronounced variation was observed at HSZ with the

Table 1. Mean concentration and standard deviation (Mean \pm SD) of SO_4^{2-} , NO_3^- , and NH_4^+ in $\text{PM}_{2.5}$, SO_2 , and NO_x with meteorological parameters at the two sites in summer in Beijing.

	CRAES (Urban site)		HSZ (Rural site)		P (t-test)
	Mean \pm SD	n	Mean \pm SD	n	
SO_4^{2-} $\mu\text{g}/\text{m}^3$	20.74 ± 20.36	614	18.23 ± 19.96	587	0.03
NO_3^- $\mu\text{g}/\text{m}^3$	8.83 ± 9.51	614	9.47 ± 11.41	587	0.29
NH_4^+ $\mu\text{g}/\text{m}^3$	10.85 ± 8.99	614	9.70 ± 8.92	499	0.03
NO_x ppb	12.89 ± 9.75	621	2.51 ± 1.90	557	< 0.01
SO_2 ppb	7.25 ± 5.32	623	1.27 ± 1.47	608	< 0.01
T $^\circ\text{C}$	26.05 ± 3.70	624	23.82 ± 3.57	619	< 0.01
RH %	62.91 ± 18.19	624	83.90 ± 15.81	619	< 0.01
Solar radiation w/m^2	97.87 ± 152.09	624	157.20 ± 233.06	619	< 0.01

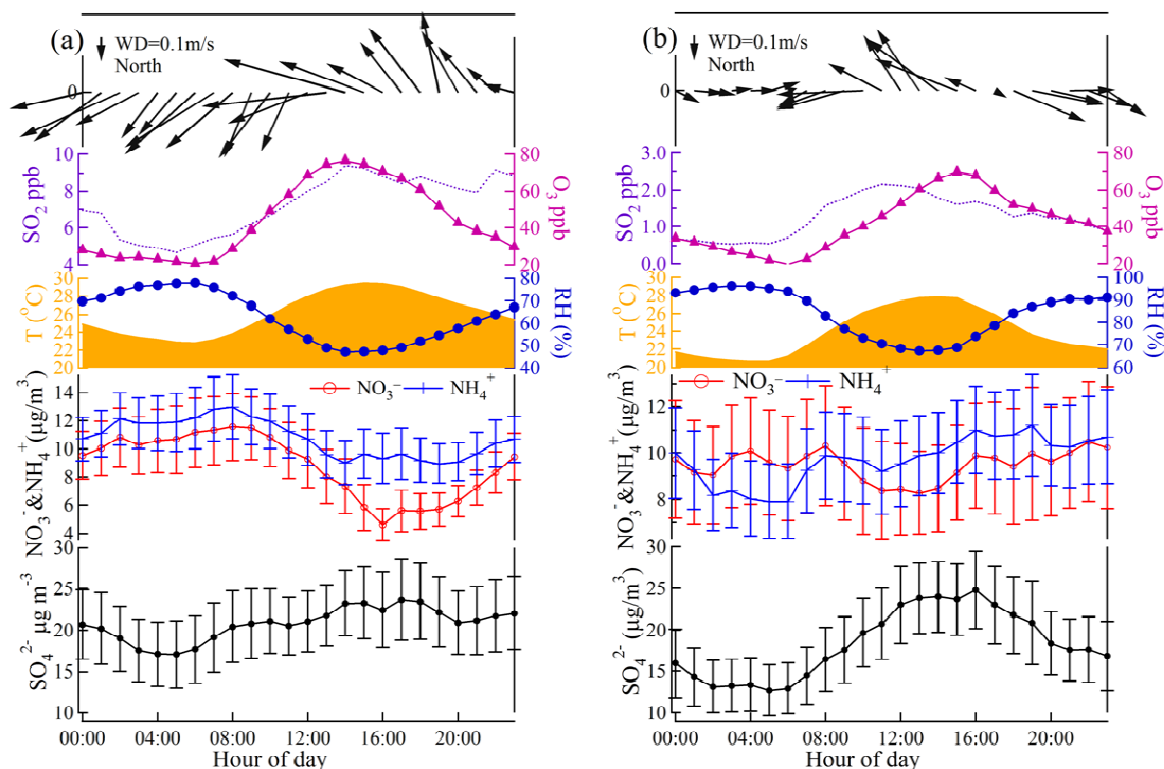


Fig. 2. Diurnal variations of SO_4^{2-} , NO_3^- , NH_4^+ , SO_2 , O_3 , temperature, RH, and wind speed and direction: (a) CRAES; (b) HSZ. Vertical bars are 1/5 standard deviations.

SO_4^{2-} concentrations from 12.71 to 24.79 $\mu\text{g}/\text{m}^3$ compared to the CRAES site (17.05 to 23.70 $\mu\text{g}/\text{m}^3$). The typical mountain-valley breeze brought the Beijing urban plume from the southeast during the afternoon and caused a more pronounced diurnal variation of SO_4^{2-} at HSZ.

Different diurnal variations of NO_3^- at the two sites are shown in Fig. 2. At the urban site, NO_3^- showed the highest peak in the early morning and the lowest value in the late afternoon. The maximum concentration of NO_3^- (11.56 $\mu\text{g}/\text{m}^3$) occurred at approximately 8:00 due to the formation and accumulation of NH_4NO_3 under high RH before sunrise. The minimum concentration of NO_3^- (4.62 $\mu\text{g}/\text{m}^3$) at approximately 16:00 was attributed to the dissociation of NH_4NO_3 with the increase of temperature. This typical diurnal pattern was widely observed in other studies (e.g., Hu *et al.*, 2008; Wu *et al.*, 2009). However, at HSZ, NO_3^- did not show a low concentration in the afternoon. The possible reason was that the regional pollutants transported from urban Beijing and NCP overwhelmed the dissociation of NH_4NO_3 .

NH_4^+ is formed via the reactions of ammonia with sulfuric acid and nitric acid (Seinfeld and Pandis, 2006) and mostly exists in the forms of $(\text{NH}_4)_2\text{SO}_4$ and NH_4NO_3 in the aerosol. Therefore, the diurnal pattern of NH_4^+ is related to that of sulfate, nitrate or both. At CRAES, NO_3^- showed a more pronounced diurnal variation than SO_4^{2-} . Thus, NH_4^+ showed a similar diurnal variation as NO_3^- ; the peak value occurred in the morning, and the lowest value occurred in the afternoon. In contrast, at HSZ, NO_3^- showed a relatively stable diurnal variation, which led to the diurnal pattern of

NH_4^+ more similar to that of SO_4^{2-} .

Effectiveness of Control Measures on SO_4^{2-} , NO_3^- , and NH_4^+

To examine SO_4^{2-} , NO_3^- , and NH_4^+ pollution during the Olympics, the campaign at the urban site from July 11 to August 24 was divided into three periods based on the periods of the source control measures and the Olympics: before the full-scale control (period 1, July 11–19), after the full-scale control but before the Olympics (period 2, July 20 to August 8), and during the Olympics (period 3, August 9–24). The concentrations of SO_4^{2-} , NO_3^- , and NH_4^+ in these three periods are compared in Fig. 3. The average concentrations of SO_4^{2-} , NO_3^- , and NH_4^+ were 24.73, 10.82, and 16.92 $\mu\text{g}/\text{m}^3$ in period 1; 42.29, 15.15, and 20.47 $\mu\text{g}/\text{m}^3$ in period 2; and 14.26, 6.45, and 7.34 $\mu\text{g}/\text{m}^3$ in period 3. Compared with those in period 1, the concentrations of SO_4^{2-} , NO_3^- , and NH_4^+ increased by 71.0%, 40.0%, and 21.0%, respectively, in period 2 but decreased by 42.3%, 40.4%, and 56.6%, respectively, in period 3. In period 2, when the full-scale control came into effect, the concentrations of SO_4^{2-} , NO_3^- , and NH_4^+ were expected to be reduced when compared with the data before the full-scale control. However, opposite results were obtained. Less rainfall and more frequent wind flow from the south-southeast sector was suggested to be the major contributor to the enhanced pollutant concentrations in period 2 (Wang *et al.*, 2010b). In this study, to further identify the impacts of source regions on the SO_4^{2-} , NO_3^- , and NH_4^+ concentrations, five-day backward trajectories, with the endpoint at 100 m

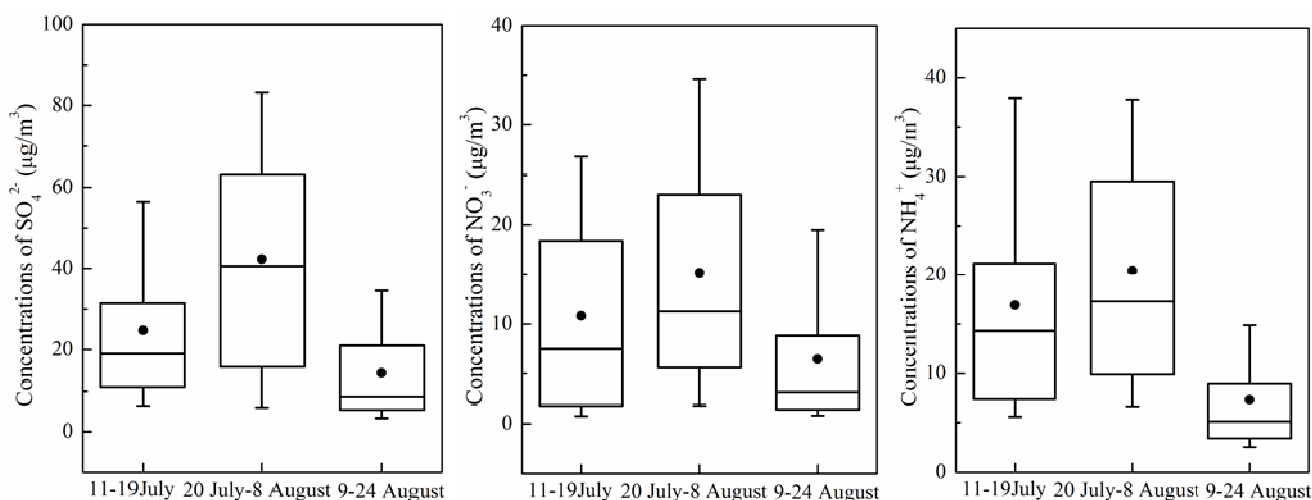


Fig. 3. Concentrations of SO_4^{2-} , NO_3^- , and NH_4^+ in three periods for all data at CRAES.

above the CRAES ground level ($40^\circ 02' \text{N}$, $116^\circ 25' \text{E}$), were calculated for every hour by the Hybrid Single-Particle Lagrangian Integrated Trajectory model (HYSPPLIT, version 4.9) with the Global Data Assimilation system (GDAS) meteorological data (Draxler and Rolph, 2003). A total of 1080 trajectories were obtained. A hierarchical cluster approach was then applied using the SPSS statistical software to classify these trajectories into several different groups based on Ward's cluster method and a squared Euclidean measure. As illustrated in Fig. 4, six suitable clusters were obtained based on the transport directions and speeds. The air masses from the south (cluster 1) and southeast (cluster 2) were dominant and accounted for 35% and 39% of the total trajectories, respectively. Northeast air masses (cluster 6) accounted for approximately 10%. Air masses, which generally originated from northwestern China and travelled faster at a higher altitude, were classified into 3 categories of clusters 3, 4, and 5, and altogether they accounted for 16%. The hourly SO_4^{2-} , NO_3^- , and NH_4^+ concentrations with clusters at the CRAES site are plotted in Fig. 5. The highest concentrations of pollutants were observed in cluster 1, which passed through the areas south of Beijing with high emissions (Shandong, Hebei, and Tianjin), followed by cluster 2. Other clusters showed lower levels of pollutants. These results were consistent with some previous studies (Streets *et al.*, 2007; Huang *et al.*, 2010; Sun *et al.*, 2010). In period 2, the high concentrations of SO_4^{2-} , NO_3^- , and NH_4^+ were attributed to frequent southerly air masses (the sum of cluster 1 and 2) that accounted for approximately 94% of the total trajectories, whereas the southerly air masses contributed to 57% in period 1 and 56% in period 3. Therefore, the air masses played an important role in the highly variable concentrations of SO_4^{2-} , NO_3^- , and NH_4^+ .

The significant impacts by the meteorological factors and regional transport make it a vague picture on the effectiveness of control measures. To minimize the influences of these factors and better evaluate the effectiveness of the control measures, we selected samples with the following criteria: (1) air masses from the northwest-north-northeast sector (270° – 360° and 0° – 45°) with wind speed below 1

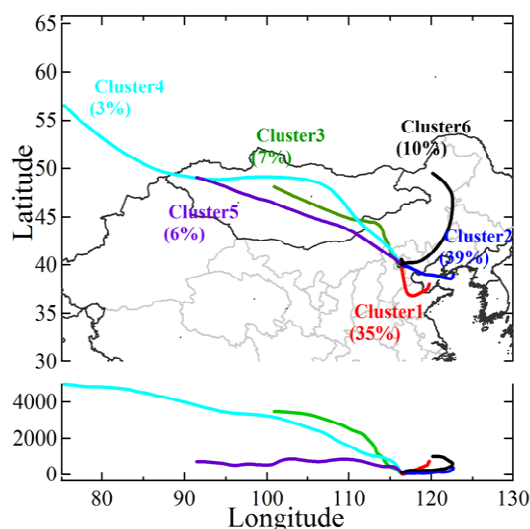


Fig. 4. Mean backward trajectories for six clusters arriving at CRAES in Beijing.

m/s were selected to avoid obvious regional pollution, and (2) rainy days were excluded due to the cleaning effect. Under these criteria, 77, 71, and 86 hourly samples were identified in the three periods, respectively, during which local emission was considered as the dominant contributor to the pollutants of the urban site. Fig. 6 illustrates the SO_4^{2-} , NO_3^- , and NH_4^+ concentrations for selected samples at CRAES in the three periods. These three species showed apparent decreases. Compared to those in period 1, SO_4^{2-} , NO_3^- , and NH_4^+ reduced by 55.6%, 38.7%, and 35.3%, respectively, in period 2 and 61.4%, 66.1%, and 69.0%, respectively, in period 3, suggesting that the control measures were effective in reducing the local secondary inorganic aerosols. Together with our previous study (Wang *et al.*, 2010b), these results indicated the important roles of both meteorological factors and control measures in the observed significant reduction of pollution during the Olympics. However, a more quantitative conclusion would require further modeling in future studies.

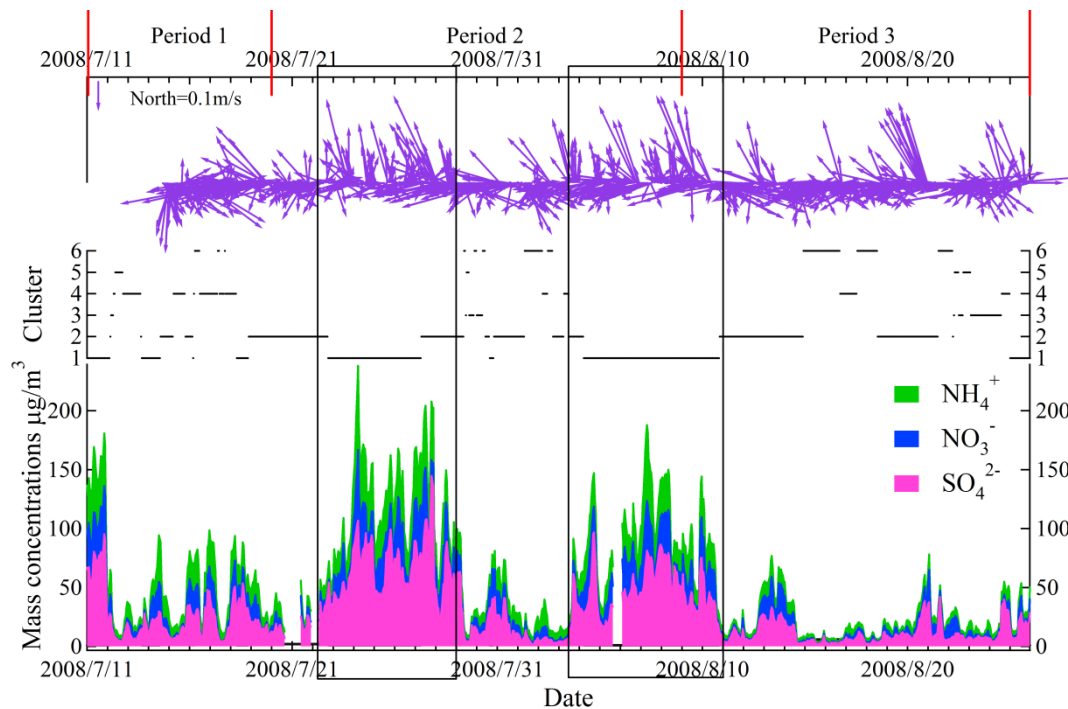


Fig. 5. Time series of SO_4^{2-} , NO_3^- , and NH_4^+ with clusters, wind speed and direction at CRAES.

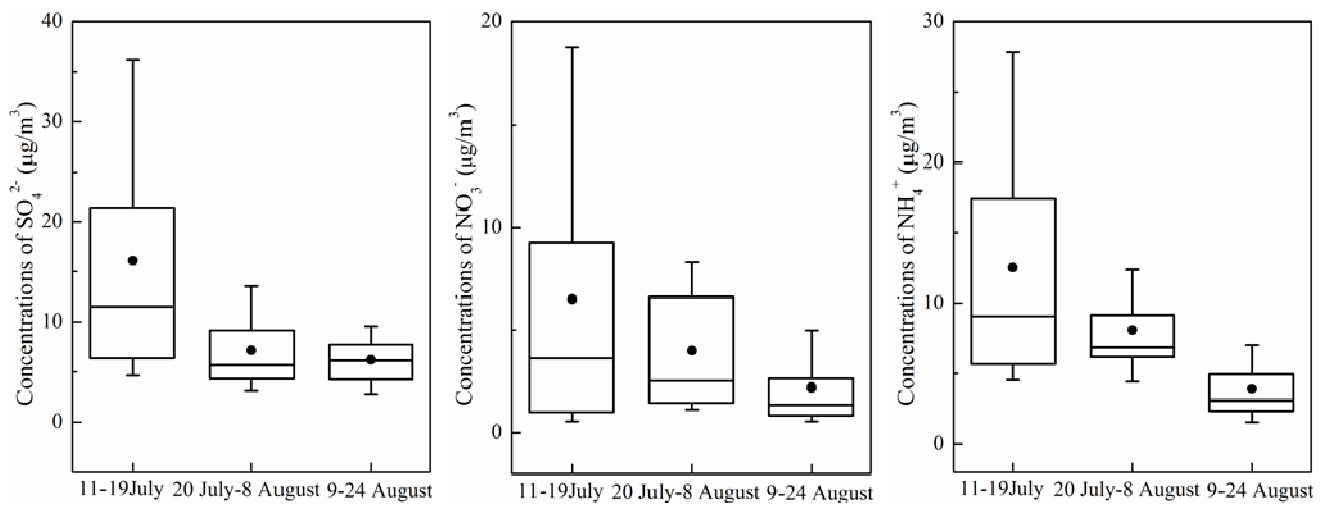


Fig. 6. Concentrations of SO_4^{2-} , NO_3^- , and NH_4^+ for selected data in three periods at CRAES.

Regional Contributions to SO_4^{2-} , NO_3^- , and NH_4^+ Pollution at the Rural Site (HSZ)

During the campaign, a heavy pollution episode was observed during August 3–10 with high loadings of SO_4^{2-} , NO_3^- , and NH_4^+ (Fig. 7). SNA (defined as the sum of SO_4^{2-} , NO_3^- , and NH_4^+) increased quickly from very low concentrations (lower than $10 \mu\text{g}/\text{m}^3$) to high concentrations (exceeding $200 \mu\text{g}/\text{m}^3$), and the average concentration (\pm standard deviation) of SNA was approximately $79.32 \pm 38.62 \mu\text{g}/\text{m}^3$ during this episode. As illustrated by the MODIS true-color image for August 4 (Fig. 8), this pollution episode not only occurred as a typical regional haze event in Beijing but also spread over a large part of the NCP. Previous studies had demonstrated that regional transport

from south of Beijing (mostly from the NCP) frequently occurred and greatly contributed to the summer Beijing pollution. Both models and field studies estimated that approximately 34%–87% for $\text{PM}_{2.5}$ (or $\text{PM}_{1.8}$) and 40%–69% for PM_{10} were attributed to sources outside Beijing (Chen *et al.*, 2007; Streets *et al.*, 2007; Guo *et al.*, 2010). For SO_4^{2-} in fine particles, the regional contribution was reported to be almost 90% (Guo *et al.*, 2010). Our previous study (Wang *et al.*, 2010b) directly examined the regional contributions to the ozone and CO pollution in Beijing via three concurrent observation sites located along an upwind-urban-downwind pathway. In the present study, the simultaneous employment of online continuous techniques for measuring the water-soluble ions at the urban site and a

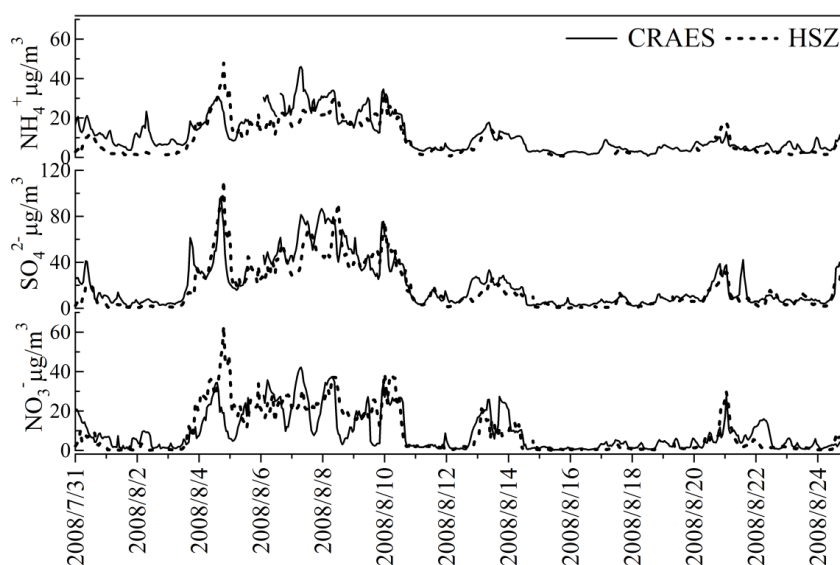


Fig. 7. The time series of SO_4^{2-} , NO_3^- , and NH_4^+ in $\text{PM}_{2.5}$ at the two sites.

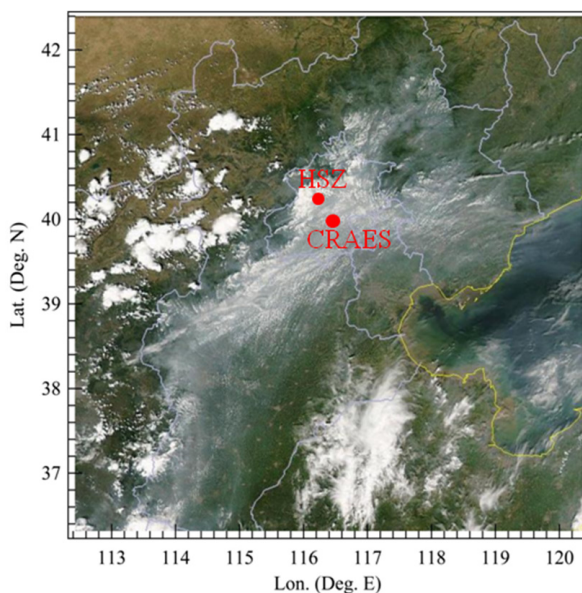


Fig. 8. MODIS true-color imagery on August 4.

downwind rural site provided a rare opportunity to directly evaluate the transport contributions to secondary aerosol species pollution. As illustrated in Fig. 7, the peaks of SO_4^{2-} , NO_3^- , and NH_4^+ at the downwind site (HSZ) appeared approximately 2–3 hours later than those at the urban site, clearly suggesting a transport contribution from the NCP and urban Beijing to the rural site.

To quantify the regional contributions of secondary aerosol species at the rural site, we selected two categories of samples to compare with the following criteria: (1) samples with the air masses from the south and the hourly concentrations of SNA exceeding $100 \mu\text{g}/\text{m}^3$ are defined as regional samples, which represent the regional air plume, and (2) samples with air masses from the northwest of HSZ are defined as local samples, which represent the clean continental air masses without obvious regional impact.

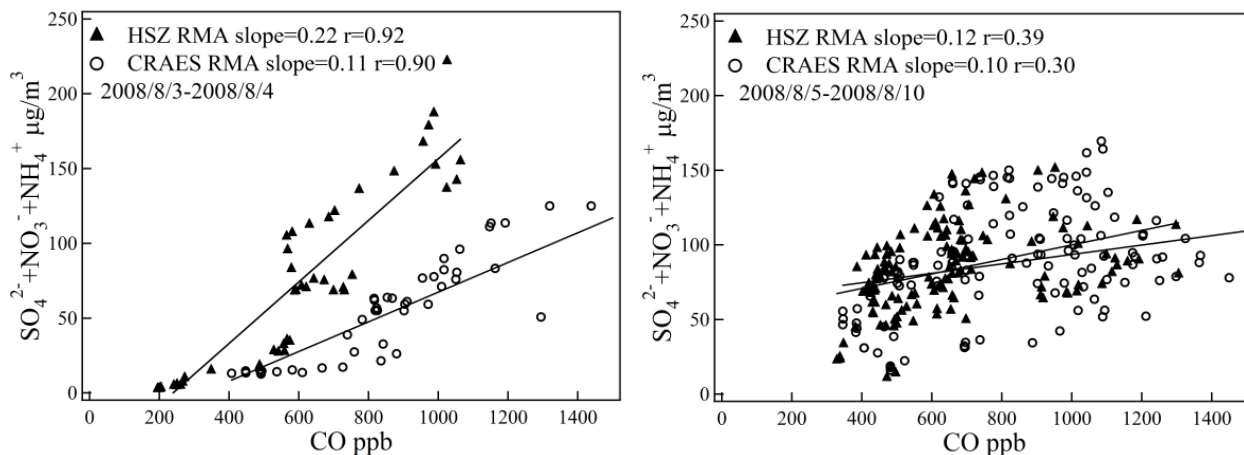
Under the above criteria, 192 samples during August 3–10 and 91 samples on August 1, 2, 22 and 23 were identified as regional and local samples, respectively. In Table 2, the concentrations of primary and secondary species are compared between the regional and local samples, and the results showed evident differences for each species. With a relative atmospheric lifetime of 1 month in summer (Xu *et al.*, 2008), CO was taken as a benchmark to evaluate the transport contributions from the North China Plain and urban Beijing to HSZ, and the result showed an increase by a factor of ~ 2 for the regional samples compared with the local samples. This increase suggested that approximately 50% of the CO at the rural site can be attributed to the transport. However, for the secondary compounds in $\text{PM}_{2.5}$, a much higher “regional/local” ratio was revealed, with 9.19 for SO_4^{2-} , 18.61 for NO_3^- , and 8.66 for NH_4^+ ; while similar levels of SO_2 and NO_x appeared in the regional and local samples. The resulting lower ratios for SO_2 and NO_x and higher ratios for secondary species (SO_4^{2-} , NO_3^- , and NH_4^+) suggested a secondary transformation during transport. It is also of interest that the regional/local ratio for NO_3^- was more than twice that of SO_4^{2-} and NH_4^+ , indicating the possible formation of NO_3^- on pre-existing aerosols instead of through the homogeneous gas-phase reaction between ammonia and nitric acid during transport (Pathak *et al.*, 2009).

To further investigate the secondary transformation processes during transport, we examined the changes in the relationship between SNA and CO at the urban site and the downwind rural site. As shown in Fig. 7, the concentrations of SO_4^{2-} , NO_3^- , and NH_4^+ rapidly increased at the beginning of this pollution episode (August 3–4) and maintained stable levels thereafter during August 5–10. Therefore, in Fig. 9, we divided the August 3–10 time period into two parts, with August 3–4 as the “growth stage” and August 5–10 as the “stabilization stage”. During the “growth stage” (August 3–4), the RMA slope of SNA versus CO was 0.22 at the rural site, approximately double that at the urban site (0.11),

Table 2. Influences of regional transport on trace gases and secondary aerosols at HSZ.

HSZ	SO ₂ ppb	NO _x ppb	CO ppm	NO ₃ ⁻ μg/m ³	SO ₄ ²⁻ μg/m ³	NH ₄ ⁺ μg/m ³
R	1.74 ± 1.58	2.56 ± 1.57	0.624 ± 0.234	21.77 ± 11.16	39.35 ± 20.77	18.19 ± 8.18
L	1.24 ± 1.69	2.43 ± 2.22	0.298 ± 0.107	1.17 ± 0.82	4.28 ± 4.06	2.10 ± 0.57
R/L	1.40	1.05	2.09	18.61	9.19	8.66

R stands for sampling on Aug. 3–10; L stands for sampling on Aug. 1, 2, 22 and 23.

**Fig. 9.** Scatter plots of SO₄²⁻ + NO₃⁻ + NH₄⁺ versus CO at the two sites.

suggesting strong secondary transformation. However, in the “stabilization stage” during August 5–10, the slope showed comparable values of 0.12 at the rural site and 0.10 at the urban site. These results suggested that secondary production mainly occurred during the growth stage of pollutant concentrations during August 3–4, and afterward (during August 5–10), the whole region experienced a stable and well-developed plume from the NCP and urban Beijing.

The foregoing discussions have demonstrated that secondary transformation during the transport from CRAES to HSZ mainly occurred in the growth stage of the episode during August 3–4. In this section, we develop a simple approach to quantify the secondary transformation contribution to the observed pollution level during August 3–4 at HSZ. The total SO₄²⁻, NO₃⁻, and NH₄⁺ concentrations at HSZ during August 3–4 can be separated into three parts depending on the type of contribution: (1) local sources (LS), (2) direct transport (DT), and (3) secondary transformation (ST). The contribution of local sources can be represented by the concentrations of SO₄²⁻, NO₃⁻, and NH₄⁺ at HSZ on August 1, 2, 22 and 23, while the direct transport contribution can be calculated by the formula $C_{i-DT} = (CO_{rural}/CO_{urban}) \times C_{i-urban}$ (where *i* stands for species of SO₄²⁻, NO₃⁻, and NH₄⁺), assuming similar levels of diffusion for CO and fine particles during the transport from CRAES to HSZ. Then, the secondary transformation contribution can be computed by deducting local sources and direct transport from the total contributions. The calculation results for LS, DT, and ST are summarized in Table 3. For the three secondary ions, the secondary transformation contribution (SO₄²⁻: 60.3%; NO₃⁻: 78.9%; NH₄⁺: 58.1%) accounted for more than half of the total

contributions, followed by direct transport and local sources, indicating the predominance of secondary transformation.

SUMMARY AND CONCLUSION

In this study, we report simultaneous online continuous measurements of SO₄²⁻, NO₃⁻, and NH₄⁺ in PM_{2.5} at an urban site and a downwind rural site in Beijing during the 29th Olympic Games. The results showed that both urban and rural areas in Beijing suffered serious secondary aerosol pollution (SO₄²⁻, NO₃⁻, and NH₄⁺) with few spatial differences in summer. Obviously diurnal variations of SO₄²⁻, NO₃⁻ and NH₄⁺ were observed at both sites and were related to the meteorological conditions, primary emissions, and regional transport. To assess the effectiveness of the control measures, the urban site sampling period was divided into three periods: before the full-scale control, after the full-scale control but before the Olympics, and during the Olympics. The high SO₄²⁻, NO₃⁻, and NH₄⁺ levels after the full-scale control resulted from the more frequent air masses from southern sectors, suggesting the importance of regional transport. After minimizing the impacts of the meteorological factors and regional transport by selecting the samples in the air masses from the sector north of Beijing, the SO₄²⁻, NO₃⁻, and NH₄⁺ concentrations were observed an obvious reduction after the full-scale control, implying that the control measures were effective in reducing the local secondary inorganic aerosols. A typical haze event, which not only occurred in Beijing but was widespread over a large part of the North China Plain, was observed during August 3–10. We separated this event into a growth stage (August 3–4) and a stable stage (August 5–10) according to different characteristics of the SNA (the

Table 3. Contributions to the rural SO_4^{2-} , NO_3^- , and NH_4^+ concentrations during August 3–4.

	Total	LS	DT	ST
CO ppm	0.578	0.298	0.280	0
SO_4^{2-} $\mu\text{g}/\text{m}^3$	32.49	4.28 (13.2%)	8.61 (26.5%)	19.60 (60.3%)
NO_3^- $\mu\text{g}/\text{m}^3$	21.08	1.17 (5.6%)	3.27 (15.5%)	16.64 (78.9%)
NH_4^+ $\mu\text{g}/\text{m}^3$	16.27	2.10 (12.9%)	4.72 (29.0%)	9.45 (58.1%)

sum of SO_4^{2-} , NO_3^- , and NH_4^+) versus CO. During the growth stage, secondary transformation evidently occurred and contributed more than half of the rural secondary species concentrations, and the whole region then experienced a stable and well-developed plume.

ACKNOWLEDGMENTS

The authors would like to acknowledge Steven Poon and Xu Pengju for their help in organizing the field study and setting up the instruments and Wang Linlin, Shou Youping, Xu Zheng, Yu Yangchun and Zhou Shengzhen for their assistance in the laboratory analysis. The HYSPLIT model was provided by the NOAA Air Resources Laboratory. This study was funded by the National Basic Research Program of China (973 Project No. 2005CB422203), Shandong Provincial Environmental Protection Department (2006045), and the Hong Kong Polytechnic University's Niche Area Development Scheme (1-BB94). Thanks to Dr. Edward C. Mignot, Shandong University, for linguistic advice.

REFERENCES

- Chan, C.K. and Yao, X.H. (2008). Air Pollution in Mega Cities in China. *Atmos. Environ.* 42: 1–42.
- Chen, D.S., Cheng, S.Y., Liu, L., Chen, T. and Guo, X.R. (2007). An Integrated MM5-CMAQ Modeling Approach for Assessing Trans-Boundary PM_{10} Contribution to the Host City of 2008 Olympic Summer Games-Beijing, China. *Atmos. Environ.* 41: 1237–1250.
- Deshmukh, D.K., Deb M.K., Tsai Y.I. and Mkoma S.L. (2011). Water-soluble Ions in $\text{PM}_{2.5}$ and PM_1 Aerosol in Durg City, Chhattisgarh, India. *Aerosol Air Qual. Res.* 11: 696–708.
- Draxler, R.R. and Rolph, G.D. (2003). HYSPLIT (Hybrid Single-Particle Lagrangian Integrated Trajectory) Model Access via NOAA ARL READY Website, NOAA Air Resources Laboratory, Silver Spring, MD. Available at: <http://www.arl.noaa.gov/HYSPLIT.php> (Accessed 2009).
- Duan, F.K., He, K.B., Ma, Y.L., Yang, F.M., Yu, S.H., Cadle, S.H., Chan, T. and Mulawa, P.A. (2006). Concentration and Chemical Characteristics of $\text{PM}_{2.5}$ in Beijing, China: 2001–2002. *Atmos. Environ.* 35: 264–275.
- Gao, X.M., Yang, L.X., Cheng, S.H., Gao, R., Zhou, Y., Xue, L.K., Shou, Y.P., Wang, J., Wang, X.F., Nie, W., Xu, P.J. and Wang, W.X. (2011). Semi-Continuous Measurement of Water-Soluble Ions in $\text{PM}_{2.5}$ in Jinan, China: Temporal Variations and Source Apportionments. *Atmos. Environ.* 45: 6048–6056.
- Guo, S., Hu, M., Wang, Z.B., Slanina, J. and Zhao, Y.L. (2010). Size-Resolved Aerosol Water-Soluble Ionic Compositions in the Summer of Beijing: Implication of Regional Secondary Formation. *Atmos. Chem. Phys.* 10: 947–959.
- He, K.B., Yang, F.M., Ma, Y.L., Zhang, Q., Yao, X.H., Chan, C.K., Cadle, S., Chan, T. and Mulawa, P. (2001). The Characteristics of $\text{PM}_{2.5}$ in Beijing, China. *Atmos. Environ.* 35: 4959–4970.
- Hu, M., Wu, Z.J., Slanina, J., Lin, P., Liu, S. and Zeng, L.M. (2008). Acidic Gases, Ammonia and Water-Soluble Ions in $\text{PM}_{2.5}$ at a Coastal Site in the Pearl River Delta, China. *Atmos. Environ.* 42: 6310–6320.
- Huang, X.F., He, L.Y., Hu, M., Canagaratna, M.R., Sun, Y., Zhang, Q., Zhu, T., Liu, A.G., Zhang, Y.H., Jayne, J.T., Ng, N.L. and Worsnop, D.R. (2010). Highly Time-Resolved Chemical Characterization of Atmospheric Submicron Particles during 2008 Beijing Olympic Games Using an Aerodyne High-Resolution Aerosol Mass Spectrometer. *Atmos. Chem. Phys.* 10: 8933–8945.
- Hughes, L.S., Cass, G.R., Gone, J., Ames, M. and Olmez, I. (1998). Physical and Chemical Characterization of Atmospheric Ultrafine Particles in the Los Angeles Area. *Environ. Sci. Technol.* 32: 1153–1161.
- Nie, W., Wang, T., Gao, X.M., Pathak, R.K., Wang, X.F., Gao, R., Zhang, Q.Z., Yang, L.X. and Wang, W.X. (2010). Comparison among Filter-Based, Impactor-Based and Continuous Techniques for Measuring Atmospheric Fine Sulfate and Nitrate. *Atmos. Environ.* 44: 4396–4403.
- Ocskay, R., Salma, I., Wang, W. and Maenhaut, W. (2006). Characterization and Diurnal Variation of Size-Resolved Inorganic Water-Soluble Ions at a Rural Background Site. *J. Environ. Monit.* 8: 300–306.
- Okuda, T., Matsuura, S., Yamaguchi, D., Umemura, T., Hnada, E., Orihara, H., Tanaka, S., He, K.B., Ma, Y.L., Cheng, Y. and Liang, L.L. (2011). The Impact of the Pollution Control Measures for the 2008 Beijing Olympic Games on the Chemical Composition of Aerosols. *Atmos. Environ.* 45: 2789–2794.
- Pathak, P.K., Wu, W.S. and Wang, T. (2009). Summertime $\text{PM}_{2.5}$ Ionic Species in Four Major Cities of China: Nitrate Formation in an Ammonia-Deficient Atmosphere. *Atmos. Chem. Phys.* 9: 1711–1722.
- Seinfeld J.H. and Pandis S.N. (2006). *Atmospheric Chemistry and Physics-From Air Pollution to Climate Change*, 2nd ed, John Wiley & Sons, Inc., New York.
- Sloane, C.S., Watson, J., Chow, J., Pritchett, L. and Richards, L.W. (1991). Size-Segregated Fine Particle Measurements by Chemical Species and Their Impact on Visibility Impairment in Denver. *Atmos. Environ. Part A* 25: 1013–1024.
- Streets, D.G., Fu, J.S., Jang, C.J., Hao, J.M., He, K.B., Tang, X.Y., Zhang, Y.H., Wang, Z.F., Li, Z.P., Zhang,

- Q., Wang, L.T., Wang, B.Y. and Yu, C. (2007). Air Quality during the 2008 Beijing Olympic Games. *Atmos. Environ.* 41: 480–492.
- Sun, J.Y., Zhang, Q., Canagaratna, M.R., Zhang, Y.M., Ng, N.L., Sun, Y.L., Jayne, J.T., Zhang, X.C., Zhang, X.Y. and Worsnop, D.R. (2010). Highly Time- and Size-Resolved Characterization of Submicron Aerosol Particles in Beijing Using an Aerodyne Aerosol Mass Spectrometer. *Atmos. Environ.* 44: 131–140.
- Sun, Y.L., Zhuang, G.S., Tang, A.H., Wang, Y. and An, Z.S. (2006). Chemical Characteristics of PM_{2.5} and PM₁₀ in Haze-Fog Episodes in Beijing. *Environ. Sci. Technol.* 40: 3148–3155.
- Takegawa, N., Miyakawa, T., Kuwata, M., Kondo, Y., Zhao, Y., Han, S., Kita, K., Miyazaki, Y., Deng, Z., Xiao, R., Hu, M., Van Pinxteren, D., Herrmann, H., Hofzumahaus, A., Holland, F., Wahner, A., Blake, D.R., Sugimoto, N. and Zhu, T. (2009). Variability of Submicron Aerosol Observed at a Rural Site in Beijing in the Summer of 2006. *J. Geophys. Res.* 114: D00G05, doi: 10.1029/2008JD010857.
- UNEP, United Nations Environmental Programme (2009). Independent Environmental Assessment Beijing 2008 Olympic Games, Nairobi, Kenya, Online Available at http://www.unep.org/publications/UNEP-eBooks/BeijingReport_ebook.pdf, Last Access: March 2010.
- Wang, H.L., Zhuang, Y.H., Wang, Y., Sun, Y.L., Yuan, H., Zhuang, G.S. and Hao, Z.P. (2008). Long-Term Monitoring and Source Apportionment of PM_{2.5}/PM₁₀ in Beijing, China. *Atmos. Environ.* 20: 1323–1327.
- Wang, M., Zhu, T., Zheng, J., Zhang, R.Y., Zhang, S.Q., Xie, X.X., Han, Y.Q. and Li, Y. (2009a). Use of a Mobile Laboratory to Evaluate Changes in On-Road Air Pollutants during the Beijing 2008 Summer Olympics. *Atmos. Chem. Phys.* 9: 8247–8263.
- Wang, S.X., Zhao, M., Xing, J., Wu, Y., Zhou, Y., Lei, Y., He, K.B., Fu, L.X. and Hao, J.M. (2010a). Quantifying the Air Pollutants Emission Reduction during the 2008 Olympic Games in Beijing. *Environ. Sci. Technol.* 44: 2490–2496.
- Wang, T., Nie, W., Gao, J., Xue, L.K., Gao, X.M., Wang, X.F., Qiu, J., Poon, C.N., Meinardi, S., Blake, D., Wang, S.L., Ding, A.J., Chai, F.H., Zhang, Q.Z. and Wang, W.X. (2010b). Air Quality during the 2008 Beijing Olympics: Secondary Pollutants and Regional Impact. *Atmos. Chem. Phys.* 10: 7603–7615.
- Wang, W.T., Primbs, T., Tao, S. and Simonich, S.L.M. (2009c). Atmospheric Particulate Matter Pollution during the 2008 Beijing Olympics. *Environ. Sci. Technol.* 43: 5314–5320.
- Wang, Y., Zhuang, G.S., Tang, A.H., Yuan, H., Sun, Y.L., Chen, S. and Zheng, A.H. (2005). The Ion Chemistry and the Source of PM_{2.5} Aerosol in Beijing. *Atmos. Environ.* 39: 3771–3784.
- Wang, Y., Hao, J., McElroy, M.B., Munger, J.W., Ma, H., Chen, D. and Nielsen, C.P. (2009b). Ozone Air Quality during the 2008 Beijing Olympics: Effectiveness of Emission Restrictions. *Atmos. Chem. Phys.* 9: 5237–5251.
- Witte, J.C., Schoeberl, M.R., Douglass, A.R., Gleason, J.F., Krotkov, N.A., Gille, J.C., Pickering, K.E. and Livesey, N. (2009). Satellite Observations of Changes in Air Quality during the 2008 Beijing Olympics and Paralympics. *Geophys. Res. Lett.* 36: L17803, doi: 10.1029/2009GL039236.
- Wu, W.S. and Wang, T. (2007). On the Performance of a Semi-Continuous PM_{2.5} Sulphate and Nitrate Instrument under High Loadings of Particulate and Sulphur Dioxide. *Atmos. Environ.* 41: 5442–5451.
- Wu, Z.J., Hu, M., Shao, K.S. and Slanina, J. (2009). Acidic Gases, NH₃ and Secondary Inorganic Ions in PM₁₀ during Summertime in Beijing, China and Their Relation to Air Mass History. *Chemosphere* 76: 1028–1035.
- Xing, J., Zhang, Y., Wang, S.X., Liu, X.H., Cheng, S.H., Zhang, Q., Chen, Y.S., Streets, D.G., Jang, A., Hao, J.M. and Wang, W.X. (2011). Modeling Study on the Air Quality Impacts from Emission Reductions and Atypical Meteorological Conditions during the 2008 Beijing Olympics. *Atmos. Environ.* 45: 1786–1798.
- Xu, J., Zhang, Y.H., Fu, J.S., Zheng, S.Q. and Wang, W. (2008). Process Analysis of Typical Summertime Ozone Episodes over the Beijing Area. *Sci. Total Environ.* 399: 147–157.
- Yang, F., Tan, J., Zhao, Q., Du, Z., He, K., Ma, Y., Duan, F., Chen, G. and Zhao, Q. (2011). Characteristics of PM_{2.5} Speciation in Representative Megacities and across China. *Atmos. Chem. Phys.* 11: 5207–5219.
- Yao, X.H., Chan, C.K., Fang, M., Cadle, S., Chan, T., Mulawa, P., He, K.B. and Ye, B.M. (2002). The water-Soluble Ionic Composition of PM_{2.5} in Shanghai and Beijing, China. *Atmos. Environ.* 36: 4223–4234.
- Zhang, Q., Jimenez, J.L., Canagaratna, M.R., Allan, J.D., Coe, H., Ulbrich, I., Alfarra, M.R., Takami, A., Middlebrook, A.M., Sun, Y.L., Dzepina, K., Dunlea, E., Docherty, K. and Decarlo, P.F. (2007). Ubiquity and Dominance of Oxygenated Species in Organic Aerosols in Anthropogenically-Influenced Northern Hemisphere Midlatitudes. *Geophys. Res. Lett.* 34: L13801, doi: 10.1029/2007GL029979.
- Zhou, J.M., Zhang, R.J., Cao, J.J., Chow, J.C. and Watson, J.G. (2012). Carbonaceous and Ionic Components of Atmospheric Fine Particles in Beijing and Their Impact on Atmospheric Visibility. *Aerosol Air Qual. Res.* 12: 492–502.
- Zhou, Y., Wu, Y., Yang, L., Fu, L.X., He, K.B., Wang, S.X., Hao, J.M., Chen, J.C. and Li, C.Y. (2010a). The Impact of Transportation Control Measures on Emission Reductions during the 2008 Olympic Games in Beijing, China. *Atmos. Environ.* 44: 285–293.
- Zhou, Y., Wang, T., Gao, X.M., Xue, L.K., Wang, X.F., Wang, Z., Gao, J., Zhang, Q.Z. and Wang, W.X. (2010b). Continuous Observations of Water-Soluble Ions in PM_{2.5} at Mount Tai (1534 m.a.s.l.) in Central-Eastern China. *J. Atmos. Chem.* 64: 107–127.

Received for review, April 12, 2012

Accepted, July 21, 2012